ments were made was leached in concentrated HCl to remove small amounts of iron contamination, washed, and dried. Wet chemical analysis indicated 600 ppm of residual iron. The commercial silica catalyst carrier was tested after being crushed by mortar and pestle to minus 100-mesh powder, while the silica gel was tested as-received.

Nitrogen gas, flowing at 150 cm^3/min, was bypassed around the hexane sparger and connected directly to the atmosphere tube. Fifty-mg silica samples were heated in the TGA at 10°C/min to 500°C, held for 3 hours, cooled to 250°C, and weighed. Nitrogen gas was then passed through the sparger, and the resulting gas mixture (5.9% hexane) was passed over the silica. Gravimetric measurements indicated that the carrier gas was saturated with *n*-hexane at 0°C, at hexane partial pressure of 6.07 kN/m^2. Samples were cooled at a rate of 2°C/min and continuously weighed.

RESULTS

Specific surface measurements for milling times up to 46 hours are presented in Figure 1. In 5 hours of milling, 50 m^2/g specific surface was obtained. The end product (after 46 hours of grinding) had a specific surface of 115.6 m^2/g and was used for hexane adsorption tests.

Figure 2 presents the *n*-hexane adsorption measurements for the three materials investigated. Adsorbent capacities of each are compared on a unit surface basis. The effect of carrier gas flow and cooling rates on the amount of hexane adsorbed was determined by varying these rates as much as 100%. No change in the amount of hexane adsorbed was measured, indicating that equilibrium values were obtained. Attrition-ground and catalyst carrier silica exhibited similar hexane adsorption capacities per unit surface. The silica gel, however, exhibited a significantly higher adsorption capacity than the other two materials, which was attributed to a different concentration of hydroxyl groups on its surface.

CONCLUSION

It has thus been demonstrated that, in addition to chemically precipitated and naturally occurring solid materials, attrition-milled solids have sufficiently large active specific surface to make them suitable for use as adsorbents. It is also quite possible that high surface solids produced by attrition milling would be useful as catalyst and catalyst carrier materials.

LITERATURE CITED

Feld, I. L., and B. H. Clemmons, Process for Wet Grinding Solids to Extreme Fineness, U.S. Pat. 3,075,710 (Jan., 1963).

Stanley, D. A., L. Y. Sadler, III, and D. R. Brooks, "Size Reduction of Ceramic Powders by Attrition Milling," in *An Intern. Conf. on Particle Technology*, IIT Research Inst., Chicago (1973).

Manuscript received October 9, 1973; revision received and accepted November 9, 1973.

Effect of Reaction Rate on the Openloop Stability of Chemical Reactors

W. L. LUYBEN

Department of Chemical Engineering
Lehigh University, Bethlehem, Pennsylvania 18015

The dynamic stability of chemical reactors has been extensively studied in the literature. An entire book has been devoted to the subject (Perlmutter, 1972). The effects of various design parameters, reaction kinetics, and reactor types have been explored.

Some of the most interesting dynamics and control problems have been shown to occur when exothermic, irreversible reactions produce the potential for openloop instability. For continuous stirred-tank reactors (CSTR), instability at a given operating level can be detected by observing the location of the roots of the characteristic equation of linearized system.

Most stability studies of CSTR's have used specific numerical examples where kinetic parameters (specific reaction rate k and activation energy E) are specified. The effects of design parameters such as heat transfer area A and coefficient U, operating temperature T, holdup volume V, throughput F, etc. have then been explored.

In some industrial reactors, the effective specific reaction rate k can be varied by operating parameters other than temperature. For example, the effective k can be changed by catalyst addition rate or by the levels of impurities in feed and recycle streams. Thus a given reactor, with fixed heat transfer area A, coefficient U, running at a constant temperature T, throughput F, and reactor volume V, can be operated with difference specific reaction rates k.

In a recent study of such a situation in an industrial reactor, some interesting results were observed. These observations are in hindsight perhaps obvious, but initially they were unexpected and surprising.

The reactor was observed to become unstable as the specific reaction rate k was reduced. With further reduc-

tion in k, the reactor once more became stable. Thus the reactor exhibited conditional stability with respect to specific reaction rate k.

Figures 1 to 4 show this effect graphically for a specific numerical case (Luyben, 1973). These plots show how the roots of the openloop characteristic equation vary as a function of the specific reaction rate k. Note that these plots are similar to classical root locus plots (in which the roots of the closedloop characteristic equation are plotted as a function of feedback controller gain K_c). However, these plots are not root locus plots since specific reaction rate k is the parameter along the loci, not controller gain K_c.

The four figures represent different heat transfer areas A. For an A of 125, in the numerical example, the openloop roots lie in the left half of the s-plane for all values of k. The reactor is therefore openloop stable for all values of k.

As area is reduced to 62.5 and less, the reactor becomes openloop unstable over a range of k's between k_{max} and k_{min}.

Before presenting the mathematical details of the example studied, a qualitative explanation of this conditional stability might be appropriate. Obviously, at very low values of k the reaction is so slow that it cannot run away. As k approaches zero, the reactor becomes merely a heated or cooled mixing pot which must be openloop stable.

On the other hand, at very high values of k, the reaction is so fast that the concentration of reactant in the tank C_A is so low that there is not enough reactant around to cause much of a temperature kick even if it all reacted. As k approaches infinity, the reaction becomes instantaneous. All the reactant is immediately consumed as it enters the reactor. The concentration of reactant C_A is zero. Thus the system becomes a cooled mixing pot with a constant heat input and must again be openloop stable.

In between these two stable extremes is a region in which openloop instability can occur.

The specific system studied (Luyben, 1973) is described by two nonlinear ordinary differential equations:

$$\frac{dC_A}{dt} = \frac{FC_{A0}}{V} - \frac{FC_A}{V} - kC_A \tag{1}$$

$$\frac{dT}{dt} = \frac{FT_0}{V} - \frac{FT}{V} - \frac{\lambda kC_A}{\rho C_p} - \frac{UA}{V\rho C_p}(T - T_J) \tag{2}$$

where

$$k = \alpha \exp(-E/RT) \tag{3}$$

Linearization for local stability analysis gives two linear ordinary differential equations:

$$\frac{dC_A}{dt} = a_{11}C_A + a_{12}T + a_{13}C_{A0} + a_{15}F \tag{4}$$

$$\frac{dT}{dt} = a_{21}C_A + a_{22}T + a_{24}T_0 + a_{25}F + a_{26}T_J \tag{5}$$

where

$$\left.\begin{aligned} a_{11} &= -\frac{\bar{F}}{V} - \bar{k} \\ a_{12} &= -\bar{C}_A E\bar{k}/R\bar{T}^2 \\ a_{21} &= -\lambda\bar{k}/\rho C_p \\ a_{22} &= \frac{-\lambda\bar{k}E\bar{C}_A}{\rho C_p R\bar{T}^2} - \frac{\bar{F}}{V} - \frac{UA}{V\rho C_p} \\ a_{26} &= \frac{UA}{V\rho C_p} \end{aligned}\right\} \tag{6}$$

The system openloop transfer function G_M between the controlled variable T and the manipulative variable T_J is

$$G_{M(s)} = \left[\frac{T}{T_J}\right]_{(s)} = \frac{a_{26}(s - a_{11})}{s^2 - (a_{11} + a_{22})s + a_{11}a_{22} - a_{12}a_{21}} \tag{7}$$

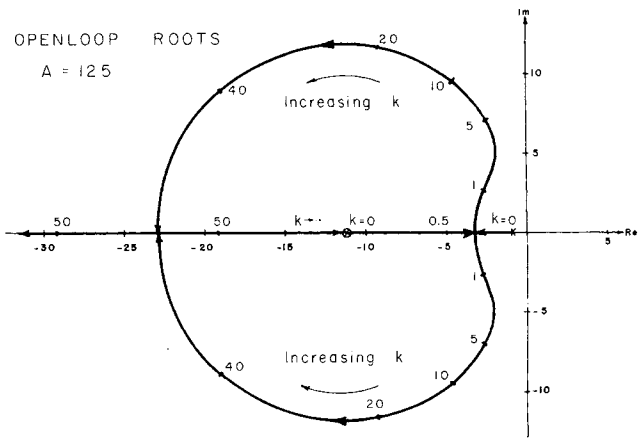

Fig 1. Effect of k on openloop roots ($A = 125$).

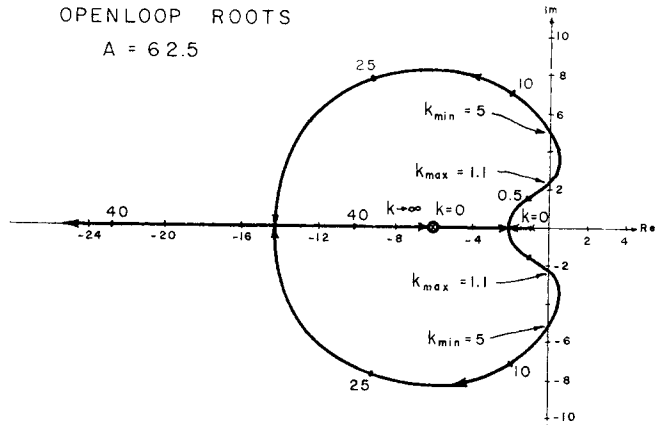

Fig. 2. Effect of k on openloop roots ($A = 62.5$).

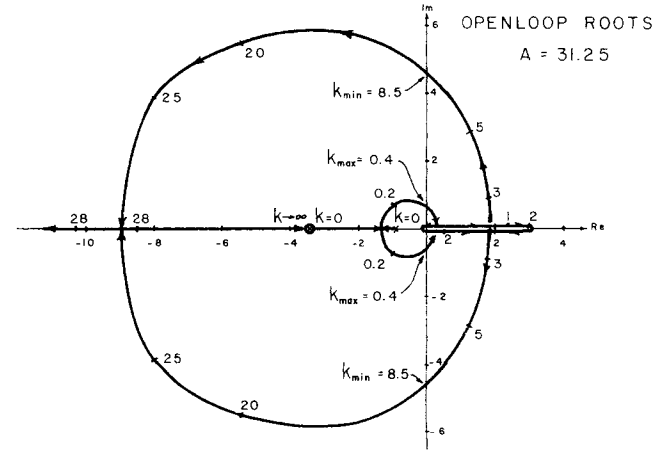

Fig. 3. Effect of k on openloop roots ($A = 31.25$).

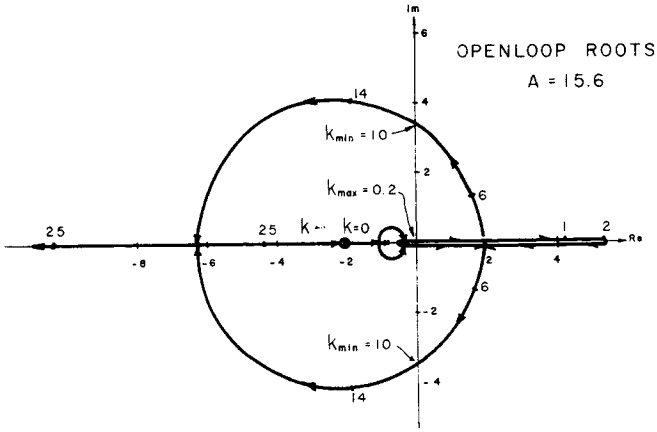

Fig. 4. Effect of k on openloop roots ($A = 15.6$).

If a proportional-only feedback controller ($B_{(s)} = K_c$) is used and two first-order lags are assumed for measurement (τ_m) and cooling-jacket (τ_J) dynamics, the closedloop characteristic equation of the system is

$$1 + B_{(s)}\,G'_{M(s)} = 1 + K_c\left[\frac{1}{\tau_M s + 1}\right]\left[\frac{1}{\tau_J s + 1}\right] G_{M(s)} \tag{8}$$

$$= 1 + K_c\left[\frac{1}{\tau_M s + 1}\right]\left[\frac{1}{\tau_J s + 1}\right]\left[\frac{a_{26}(s + a_{11})}{s^2 - (a_{11} + a_{22})s + a_{11}a_{22} - a_{12}a_{21}}\right] \tag{9}$$

$$s^4[\tau_J\tau_M] + s^3[\tau_J + \tau_M - (a_{11} + a_{22})\tau_J\tau_M] + s^2[\tau_J\tau_M(a_{11}a_{22} - a_{12}a_{21}) + 1 - (a_{11} + a_{22})(\tau_J + \tau_M)] + s[(\tau_J + \tau_M)(a_{11}a_{22} - a_{12}a_{21}) - (a_{11} + a_{22}) + K_c a_{22}] + [a_{11}a_{22} - a_{12}a_{21} - K_c a_{11}a_{22}] = 0 \tag{10}$$

Figures 1 to 4 show the effect of the specific reaction rate k on the roots of the openloop ($K_c = 0$) characteristic equation. Only the two openloop roots that vary with k are shown. There are two other constant openloop roots at $-1/\tau_M$ and $-1/\tau_J$. The contours begin at the poles of the openloop system transfer function. When $k = 0$ the two roots are at $s = -\overline{F}/V$ and $s = -\overline{F}/V - UA/V\rho C_p$. One of the contours ends at the zero of the openloop system transfer function. As k approaches infinity the openloop root approaches $s = a_{11} = -\overline{F}/V - UA/V\rho C_p$.

Notice the unusual, highly nonlinear shape of the contours, particularly the folding back of the loci along the positive real axis.

Figure 5 is a classical closedloop root locus plot that shows the effect of controller gain K_c on closedloop stability for a fixed specific reaction rate of 0.867 and area of 31.25. A τ_J of 0.033 hours and a τ_M of 0.0083 hours are used. This system is openloop unstable.

It is also closedloop unstable for values of gain below K_{min}. It again becomes closedloop unstable for gains greater than K_{max}.

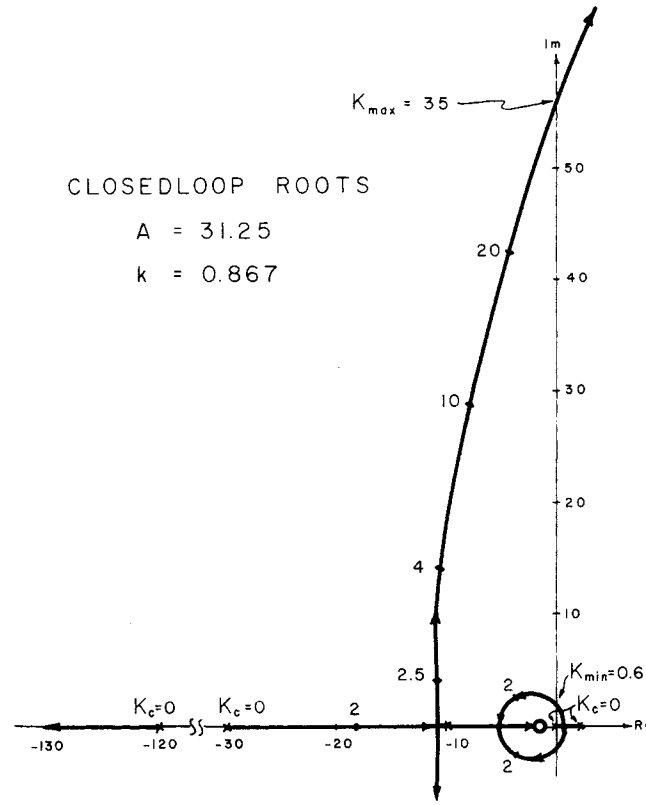

Fig. 5. Root locus plot of closedloop roots for $k = 0.867$ and $A = 31.25$.

NOTATION

a = coefficients of linearized equations
A = heat transfer area
B = feedback controller transfer function
C_A = concentration of reactant in reactor
C_{A0} = concentration of reactant in feed
C_p = heat capacity
E = activation energy
F = feed rate
G'_M = overall process openloop transfer function including measurement and jacket lags
G_M = process openloop transfer function
k = specific reaction rate
k_{max} = maximum openloop stable reaction rate
k_{min} = minimum openloop stable reaction rate
K_c = feedback controller gain
K_{max} = maximum closedloop stable gain
K_{min} = minimum closedloop stable gain
R = perfect gas constant
T = reactor temperature
T_J = cooling jacket temperature
T_0 = feed temperature
t = time
s = Laplace transform variable
U = heat transfer coefficient
V = reactor volume
α = pre-exponential factor
ρ = density
λ = heat of reaction
τ_M = time constant of measurement lag
τ_J = time constant of cooling jacket lag

Overscored variables indicate steadystate values.

LITERATURE CITED

Luyben, W. L., *Process Modeling, Simulation and Control for Chemical Engineers*, pp. 109, 226, McGraw-Hill, N. Y. (1973).

Perlmutter, D. D., *Stability of Chemical Reactors*, Prentice-Hall, Englewood Cliffs, N. J. (1972).

Manuscript received July 25, 1973, and accepted September 5, 1973.